Endothelial cell prostaglandin E$_2$ receptor EP4 is essential for blood pressure homeostasis

Hu Xu,[1,2,3] Bingying Fang,[1] Shengnan Du,[4] Sailun Wang,[1] Qingwei Li,[1] Xiao Jia,[1] Chengzhen Bao,[1] Lan Ye,[1] Xue Sui,[1] Lei Qian,[1] Zhilin Luan,[1] Guangrui Yang,[5] Feng Zheng,[1,3] Nanping Wang,[1,2,3] Lihong Chen,[1,3] Xiaoyan Zhang,[1,2,3] and Youfei Guan[1,2,3]

[1]Advanced Institute for Medical Sciences and [2]Department of Physiology and Pathophysiology, School of Basic Medical Sciences, Dalian Medical University, Dalian, China. [3]Liaoning Engineering and Technology Research Center of Nuclear Receptors and Major Metabolic Diseases, Dalian, China. [4]Department of Pharmacology, School of Basic Medical Sciences, Zhengzhou University, Zhengzhou, China. [5]School of Bioengineering, Dalian University of Technology, Dalian, China.

Prostaglandin E$_2$ and its cognate EP1–4 receptors play important roles in blood pressure (BP) regulation. Herein, we show that endothelial cell–specific (EC-specific) EP4 gene–knockout mice (EC-EP4$^{-/-}$) exhibited elevated, while EC-specific EP4-overexpression mice (EC-hEP4^{OE}) displayed reduced, BP levels compared with the control mice under both basal and high-salt diet–fed conditions. The altered BP was completely abolished by treatment with L–N^G-nitro-L-arginine methyl ester (L-NAME), a competitive inhibitor of endothelial nitric oxide synthase (eNOS). The mesenteric arteries of the EC-EP4$^{-/-}$ mice showed increased vasoconstrictive response to angiotensin II and reduced vasorelaxant response to acetylcholine, both of which were eliminated by L-NAME. Furthermore, EP4 activation significantly reduced BP levels in hypertensive rats. Mechanistically, EP4 deletion markedly decreased NO contents in blood vessels via reducing eNOS phosphorylation at Ser1177. EP4 enhanced NO production mainly through the AMPK pathway in cultured ECs. Collectively, our findings demonstrate that endothelial EP4 is essential for BP homeostasis.

Introduction

Hypertension is one of the most important public health issues worldwide because of its high incidence and severe cardiovascular outcomes. Tight control of hypertension is critical in the prevention of cardiovascular, renal, cerebrovascular, and retinal complications (1). There are many factors that regulate blood pressure (BP) mainly via affecting cardiac output, blood volume, and vascular tone. The vasculature is essential in BP regulation, and both 2 primary cell types, i.e., endothelial cells (ECs) and vascular smooth muscle cells (VSMCs), are highly involved in BP regulation (2). ECs produce nitric oxide (NO) by endothelial nitric oxide synthase (eNOS) and release it to act on VSMCs beneath the endothelium, leading to vascular relaxation and BP reduction. Usually, the phosphorylation of Thr495 by protein kinase C lowers eNOS activity and decreases NO production, while the phosphorylation of Ser1177 by AMP kinase (AMPK) or protein kinase A (PKA) promotes eNOS activity and increases NO synthesis (3, 4).

Prostaglandins (PGs) are endogenous oxygenated fatty acid metabolites catalyzed by cyclooxygenases (COXs) from arachidonic acid, including 5 major bioactive compounds, i.e., prostaglandin E$_2$ (PGE$_2$), PGF$_{2\alpha}$, PGD$_2$, prostacyclin (PGI$_2$), and thromboxane A$_2$. Increasing evidence demonstrates that PGs play critical roles in regulating vascular structure and BP. The general effects of PGs are reducing BP, consistent with the hypertensive side effect of nonsteroidal antiinflammatory drugs (NSAIDs), which block the production of PGs by inhibiting COXs (5). Among 5 PGs, PGE$_2$ is a major PG synthesized in the kidney and vasculature, where it regulates cardiovascular and renal functions through 4 distinct G protein–coupled receptors, i.e., EP1, EP2, EP3, and EP4. Each subtype exhibits a distinct function because of its characteristic tissue distribution and specific signaling pathway (6, 7). We and others have previously identified that activation of EP1 and EP3 leads to vasoconstriction, while activation of EP2 and EP4 results in vasorelaxation (8–10).

So far, most of the studies on the role of each EP receptor in regulating BP are based on the use of conventional knockout mice and/or selective ligands, with the cell type–specific effects of each EP receptor largely unclear. Our recent study has revealed that deletion of EP4 in VSMCs increases BP and promotes the incidence of aortic dissection, suggesting VSMC EP4 is essential for vascular homeostasis and remodeling (11). However, although it has been previously reported that endothelial EP4 is vital in reendothelialization after vascular injury and reestablishment of microcirculation following myocardial ischemia/reperfusion injury (12, 13), direct evidence is lacking for the role of endothelial EP4 in BP regulation.

In this study, by generating 2 genetically manipulated mouse strains in which EP4 is specifically deleted or overexpressed in ECs, combined with the use of specific EP4 agonists and/or antagonists, we found that conditional deletion of the EP4 gene in ECs increases BP, while specific overexpression of human EP4 gene in ECs decreases BP. Activation of EP4 promotes NO production by increasing the phosphorylation of eNOS at the Ser1177 residue mainly via the AMPK pathway. Collectively, our findings demonstrate, for the first time to our knowledge, that EC EP4 is essential in BP homeostasis and dysfunction of EP4 may contribute to the pathogenesis of hypertension.

Results

EP4 deletion in ECs elevates BP under basal, high-salt, and angiotensin II–infused conditions. To elucidate the role of EP4 in vascular ECs, we generated a mouse line with the EP4 gene conditionally knocked out in ECs (EC-EP4$^{-/-}$), by crossing the EP4-flox/flox mice (EP4$^{fl/fl}$) with Tie2-Cre mice (Supplemental Figure 1A; supplemental material available online with this article; https://doi.org/10.1172/jci.insight.138505DS1). PCR, real-time PCR, and en face immunofluorescence assays were used for genotyping (Supplemental Figure 1, B and C) and validating the depletion of EP4 in ECs (Supplemental Figure 1, D and E). While EP4 was almost completely depleted in vascular endothelium (Supplemental Figure 1, D and E), the aortic expression of EP1, EP2, and EP3 was not influenced (Supplemental Figure 1F).

To illustrate the role of endothelial EP4 in BP regulation, BP levels of the EC-EP4$^{-/-}$ and littermate control (EP4$^{fl/fl}$) mice were compared at baseline and after high-salt diet feeding. The EC-EP4$^{-/-}$ mice exhibited significantly higher BP than the controls under basal conditions as measured by tail cuff (Figure 1A), carotid artery intubation (Figure 1B), or radio telemetry recording (Figure 1C). Under high-salt diet feeding, both EP4$^{fl/fl}$ and EC-EP4$^{-/-}$ mice showed elevated BP, while BP levels in the EC-EP4$^{-/-}$ mice remained higher at all time points as compared with the EP4$^{fl/fl}$ mice (Figure 1D and Supplemental Figure 1, G–I), demonstrating that the EC-EP4$^{-/-}$ mice developed hypertension without increased salt sensitivity. Consistently, in an angiotensin II–induced (AngII-induced) hypertension model, BP levels in the EC-EP4$^{-/-}$ mice remained higher than the control mice throughout the 4-week treatment (Figure 1E and Supplemental Figure 1J), suggesting a comparable pressor response to AngII between the 2 genotypes. The cardiac output and urine volume were not changed by the EP4 gene deletion in ECs (Supplemental Figure 2 and Supplemental Table 1). Serum contents of several vasoactive substances, including renin, AngII, aldosterone, and PGI$_2$ metabolites, were similarly unaltered (Supplemental Figure 3, A–D). Collectively, these results demonstrate that EP4 deletion in ECs elevates BP under basal, high-salt feeding, and AngII-infused conditions. The EC-EP4$^{-/-}$ mice developed elevated BP with little change in salt and AngII sensitivity.

Endothelial EP4 deletion compromises the hypotensive effect of PGE$_2$ and agonist PGE$_1$-OH. To determine whether EC-specific deletion of EP4 alters vascular response to various vasopressors or vasodepressor agents, male EP4$^{fl/fl}$, EC-EP4$^{-/-}$, and VSMC-specific EP4-knockout (VSMC-EP4$^{-/-}$) mice (11) were anesthetized, and BP levels were measured following intravenous injection of PGE$_2$ or the EP subtype–specific agonists. The results showed that PGE$_2$ significantly reduced BP levels in the EP4$^{fl/fl}$ and VSMC-EP4$^{-/-}$ mice, with much less reduction observed in the EC-EP4$^{-/-}$ mice (Figure 1, F–H). Similarly, the EP4 selective agonist PGE$_1$-OH displayed attenuated hypotensive effect in the EC-EP4$^{-/-}$ mice compared with that in the EP4$^{fl/fl}$ and VSMC-EP4$^{-/-}$ mice (Figure 1, I–K). In contrast, infusion of sulprostone, a dual EP1/EP3 agonist, elevated BP to a similar extent in the EP4$^{fl/fl}$, VSMC-EP4$^{-/-}$, and EC-EP4$^{-/-}$ mice (Supplemental Figure 1K). Injection of the EP2 agonist butaprost also resulted in a comparable decrease in BP in all 3 groups (Supplemental Figure 1L). In addition, similar increased BP was observed after intravenous injection of AngII among the 3 genotypes (Supplemental Figure 1M). Notably, no difference in BP following PGE$_2$, PGE$_1$-OH, sulprostone, and butaprost treatment was observed between the EP4$^{fl/fl}$ mice and VSMC-EP4$^{-/-}$ mice (Figure 1, F–K; and Supplemental Figure 1, K and L). Together, these findings suggest that the hypotensive effect of PGE$_2$ is largely mediated by the EP4 receptor in ECs rather than VSMCs.
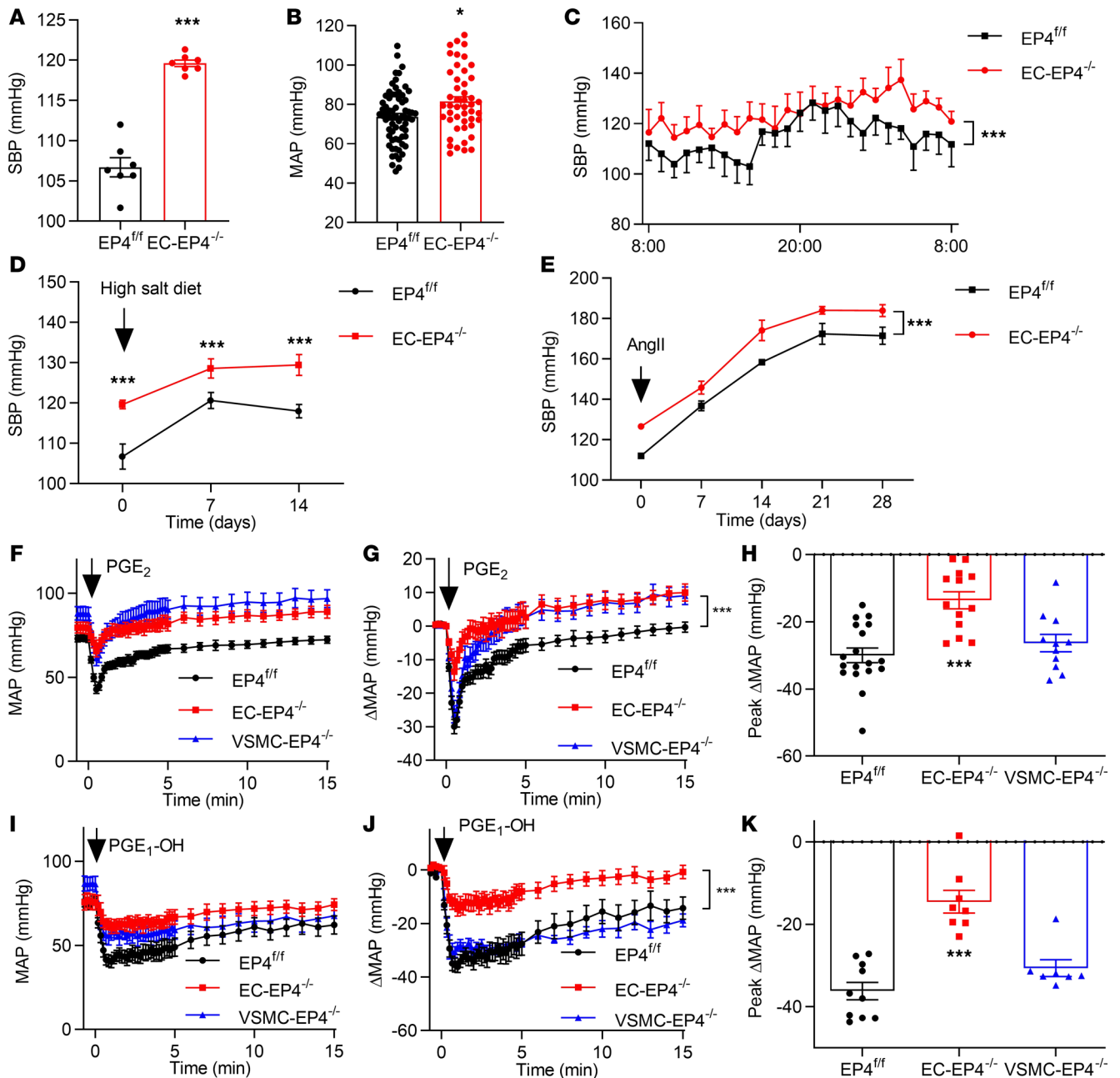
Figure 1. EP4 deletion in ECs elevates BP and compromises the hypotensive effect of PGE$_2$ and agonist PGE$_1$-OH. (**A**) Systolic BP (SBP) monitored by tail cuff in conscious EP4$^{fl/fl}$ and EC-EP4$^{-/-}$ mice. ***$P < 0.001$, $n = 7$. (**B**) Mean arterial BP (MAP) recorded by carotid arterial catheterization in anesthetized EP4$^{fl/fl}$ and EC-EP4$^{-/-}$ mice. *$P < 0.05$, $n = 47$–69. (**C**) SBP monitored by implantable radiotelemetry in conscious EP4$^{fl/fl}$ and EC-EP4$^{-/-}$ mice. ***$P < 0.001$, $n = 5$. (**D**) SBP in the EP4$^{fl/fl}$ and EC-EP4$^{-/-}$ mice with continued high-salt diet feeding for 2 weeks. ***$P < 0.001$, $n = 5$–7. (**E**) SBP in the EP4$^{fl/fl}$ and EC-EP4$^{-/-}$ mice with chronic AngII (1000 ng/kg/min) infusion for 4 weeks. ***$P < 0.001$, $n = 11$–14. (**F**) Effect of intravenous infusion of PGE$_2$ (100 μg/kg) on MAP in anesthetized EP4$^{fl/fl}$, EC-EP4$^{-/-}$, and VSMC-EP4$^{-/-}$ mice. MAP was measured by carotid arterial catheterization. (**G**) The net change of MAP after PGE$_2$ infusion. ***$P < 0.001$ vs. EP4$^{fl/fl}$, $n = 13$–18. (**H**) The maximum net change of MAP in response to PGE$_2$ infusion. ***$P < 0.001$ vs. EP4$^{fl/fl}$, $n = 13$–18. (**I**) Effect of intravenous infusion of PGE$_1$-OH (100 μg/kg) on MAP in anesthetized EP4$^{fl/fl}$, EC-EP4$^{-/-}$, and VSMC-EP4$^{-/-}$ mice as assessed by carotid arterial catheterization. (**J**) The net change of MAP after PGE$_1$-OH infusion. ***$P < 0.001$ vs. EP4$^{fl/fl}$, $n = 8$–10. (**K**) The maximum net change of MAP in response to PGE$_1$-OH infusion. ***$P < 0.001$ vs. EP4$^{fl/fl}$, $n = 8$–10. Data are represented as mean ± SEM; 2-tailed Student's t tests for **A**, **B**, and **D**; 2-way ANOVA tests for **C**, **E**, **G**, and **J**; 1-way ANOVA followed by Dunnett's multiple comparisons tests for **H** and **K**.

Reduced vascular NO production and blunted acetylcholine-induced vasorelaxation in the EC-EP4$^{-/-}$ mice. It has been well documented that impaired NO production in ECs or tolerance of NO in VSMCs leads to BP increase (14, 15). To determine whether increased BP in the EC-EP4$^{-/-}$ mice is attributable to impaired endothelial NO production, we examined the NO levels in the serum, aortas, and mesenteric
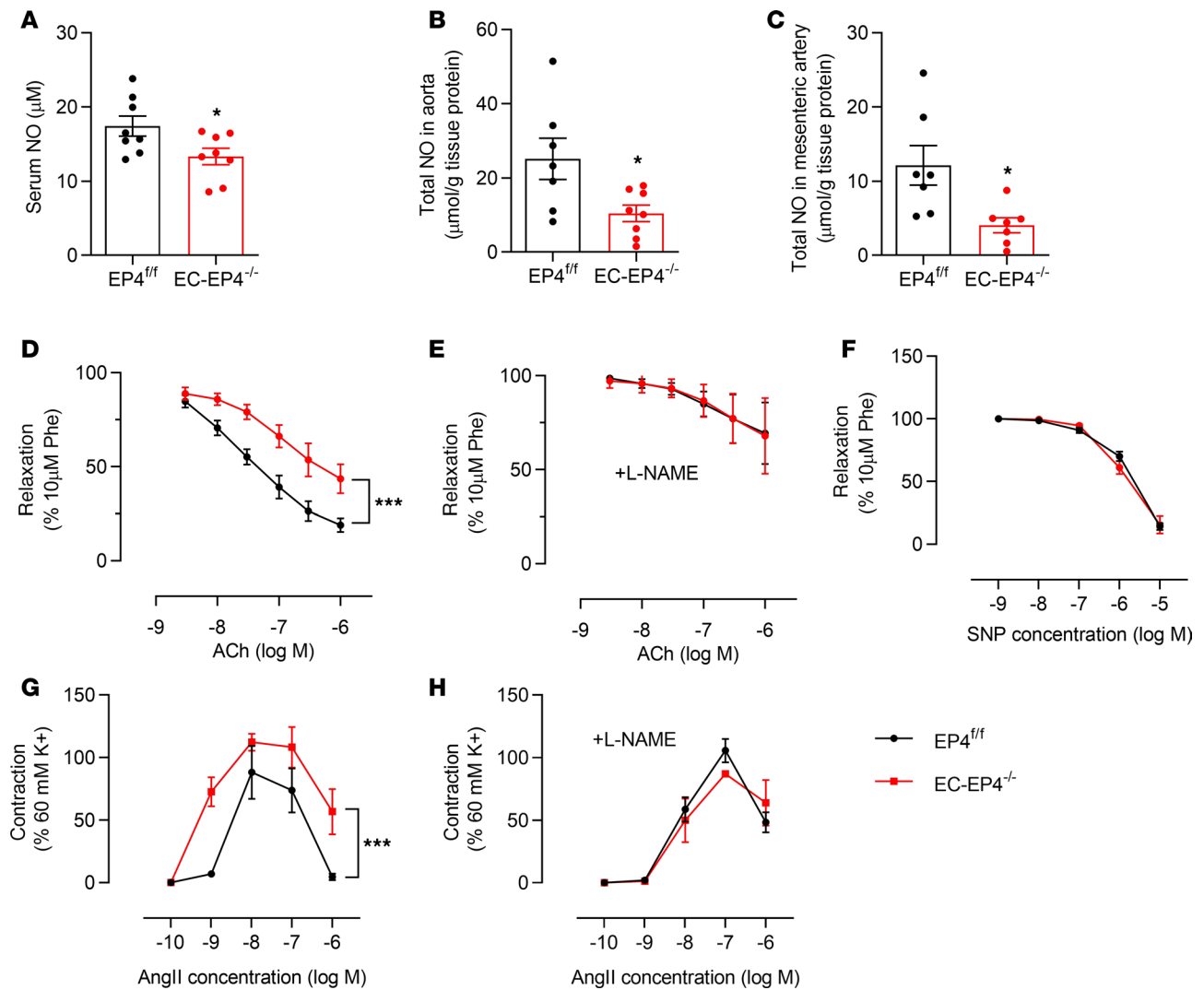
Figure 2. Reduced vascular NO production blunted acetylcholine-induced vasorelaxation and enhanced AngII-mediated vasoconstriction in the EC-EP4$^{-/-}$ mice. (A–C) The NO content in serum (A), aortas (B), and mesenteric arteries (C) of the EP4$^{fl/fl}$ and EC-EP4$^{-/-}$ mice. *$P < 0.05$, $n = 7$–8. (D and E) Vasodilatory response of the mesenteric arteries from the EP4$^{fl/fl}$ and EC-EP4$^{-/-}$ mice to acetylcholine (Ach) with (D) or without (E) preincubation of L-NAME. ***$P < 0.001$, $n = 4$. (F) Similar vasorelaxant response of the mesenteric arteries from the EP4$^{fl/fl}$ and EC-EP4$^{-/-}$ mice to SNP. $n = 8$. (G and H) Vasoconstrictive response of the mesenteric arteries to AngII with (G) or without (H) preincubation of L-NAME in the EP4$^{fl/fl}$ and EC-EP4$^{-/-}$ mice with 28-day exposure to chronic AngII infusion. ***$P < 0.001$, $n = 4$. Data are represented as mean ± SEM; 2-tailed Student's t test for A–C; 2-way ANOVA tests for D–H.

arteries. As shown in Figure 2, A–C, serum NO levels and the NO content in the aortas and mesenteric arteries were significantly decreased in the EC-EP4$^{-/-}$ mice as compared with the EP4$^{fl/fl}$ mice, suggesting that vascular capacity for producing NO was impaired in the EC-EP4$^{-/-}$ mice. In support, the acetylcholine-induced (Ach-induced) vasorelaxation was significantly attenuated in the mesenteric arteries isolated from the EC-EP4$^{-/-}$ mice (Figure 2D). Preincubation of blood vessels with L–N^G-nitro-L-arginine methyl ester (L-NAME) completely abolished the impaired response to Ach (Figure 2E). These findings support that endothelial EP4 is critical for NO biosynthesis and mediates Ach-elicited vasodilation. To determine whether the mesenteric artery of the EC-EP4$^{-/-}$ mouse has a defect in NO signaling, sodium nitroprusside (SNP), an NO donor, was used to treat the mesenteric arteries from both EP4$^{fl/fl}$ mice and EC-EP4$^{-/-}$ mice. As shown in Figure 2F, the endothelium-independent relaxation was not different between the 2 genotypes, suggesting the NO signaling pathway remained intact in the vasculature of the EC-EP4$^{-/-}$ mice. In addition, the mesenteric arteries from the EC-EP4$^{-/-}$ mice showed an increased vasoconstrictive response to AngII compared with the EP4$^{fl/fl}$ mice (Figure 2G), which was also completely eliminated by the L-NAME pretreatment (Figure 2H), suggesting that endothelial EP4 counteracts AngII-induced
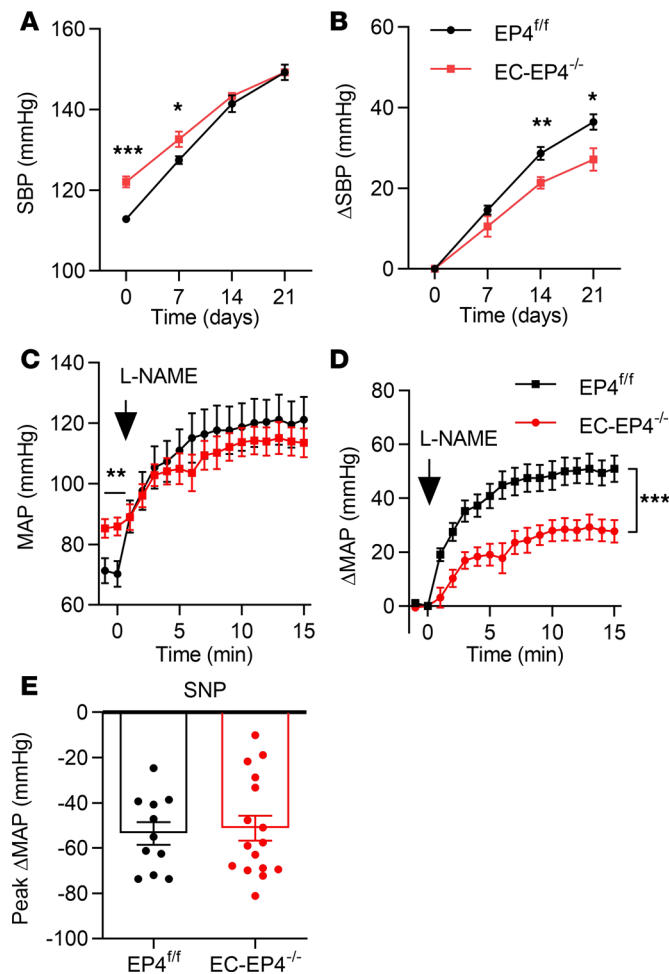
Figure 3. L-NAME treatment eliminates the difference of BP between EP4^fl/fl and EC-EP4^-/- mice. (**A** and **B**) SBP (**A**) and the net change of SBP (**B**) in the EP4^fl/fl and EC-EP4^-/- mice in response to L-NAME was monitored by tail cuff every 7 days over 3 weeks. *$P < 0.05$, **$P < 0.01$, and ***$P < 0.001$, $n = 6–7$. (**C** and **D**) Effect of intravenous injection of L-NAME (25 mg/kg) on MAP in the EP4^fl/fl and EC-EP4^-/- mice. MAP was measured by carotid arterial catheterization (**C**). The net changes of MAP were compared between 2 genotypes (**D**). ***$P < 0.001$. $n = 11$. (**E**) The maximal net change of MAP after SNP infusion in anesthetized EP4^fl/fl and EC-EP4^-/- mice. $n = 11–16$. Data are represented as mean ± SEM; 2-tailed Student's t tests for **A**–**C** and **E**; 2-way ANOVA test for **D**.

vasoconstriction in a NO-dependent manner. However, no difference in phenylephrine-evoked vasoconstriction was observed between the EP4^fl/fl and EC-EP4^-/- mice (Supplemental Figure 3E).

L-NAME eliminates the difference of BP between EP4^fl/fl and EC-EP4^-/- mice. NO produced by activated eNOS in ECs acts on its canonical receptor soluble guanylyl cyclase in VSMCs, resulting in vasodilation and BP reduction (16). To further confirm defective vascular NO production is responsible for elevated BP in the EC-EP4^-/- mice, we treated the mice with L-NAME in drinking water, a competitive inhibitor of eNOS, for 3 weeks. Although both EP4^fl/fl and EC-EP4^-/- mice exhibited continuous increase of BP, the difference of BP between the 2 genotypes was gradually abrogated as assessed by both tail-cuff and telemetry methods (Figure 3A and Supplemental Figure 3F). As expected, the net increase of BP in the EC-EP4^-/- mice was lower than that in the EP4^fl/fl mice (Figure 3B). Similarly, intravenous bolus injection of L-NAME to acutely block eNOS activity increased BP in both genotypes and completely abolished the difference of BP between EP4^fl/fl and EC-EP4^-/- mice, as assessed by carotid arterial catheterization (Figure 3, C and D). Thus, the increased BP in the EC-EP4^-/- mice likely reflects a defective NO signaling in the vasculature. However, infusion of SNP, a NO donor, led to a comparable BP drop in the EP4^fl/fl and EC-EP4^-/- mice (Figure 3E), suggesting vasodilatory response to exogenous NO remains intact in the EC-EP4^-/- mice.

Overexpression of human EP4 in ECs reduces BP under both basal and high-salt conditions. Furthermore, we used the CRISPR/Cas9 technique to generate a mouse strain with EC-specific overexpression of
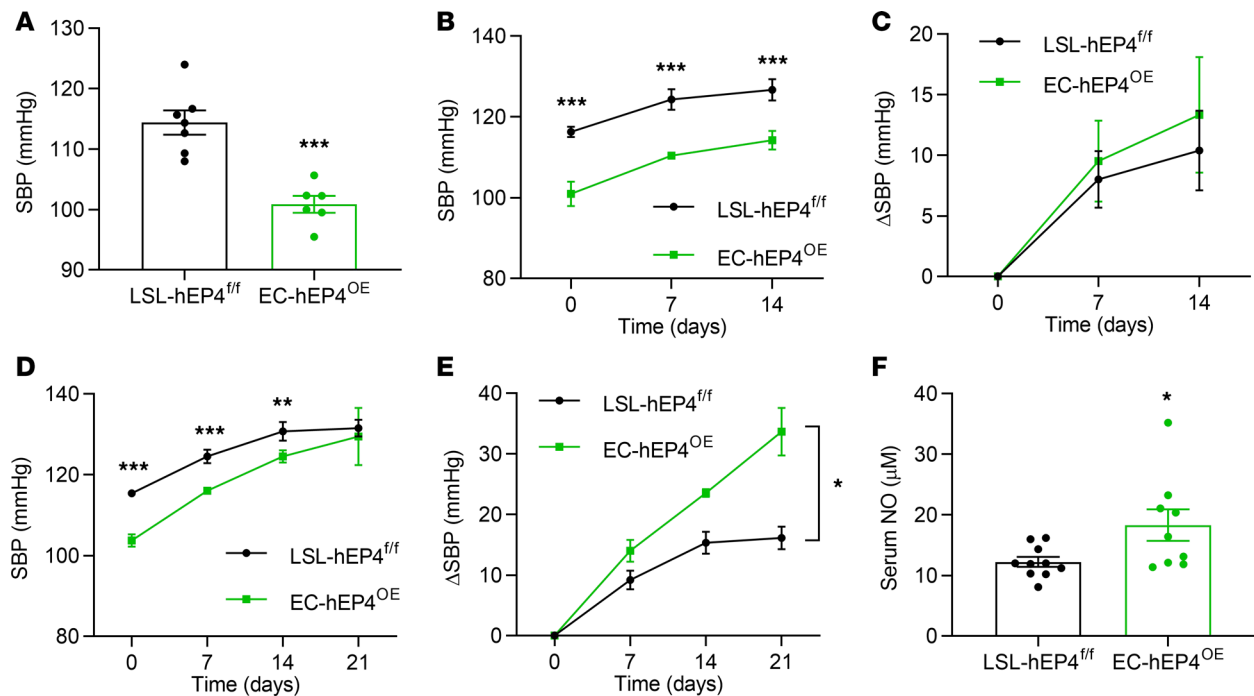
Figure 4. The EC-hEP4^{OE} mice exhibit reduced BP levels and increased serum NO concentrations. (**A**) SBP in the LSL-hEP4$^{fl/fl}$ and EC-hEP4^{OE} mice at basal conditions. ***$P < 0.001$, $n = 6$–7. (**B** and **C**) SBP (**B**) and the net change of SBP (**C**) in the LSL-hEP4$^{fl/fl}$ and EC-hEP4^{OE} mice with continuous high-salt diet feeding for 2 weeks. **$P < 0.01$, ***$P < 0.001$, $n = 6$–7. (**D** and **E**) SBP in the LSL-hEP4$^{fl/fl}$ and EC-hEP4^{OE} mice with L-NAME treatment for 3 weeks (**D**). The net changes of SBP were compared between 2 genotypes (**E**). *$P < 0.05$, and ***$P < 0.001$, $n = 5$–7. (**F**) Serum NO concentrations in the LSL-hEP4$^{fl/fl}$ and EC-hEP4^{OE} mice. *$P < 0.05$, $n = 9$–10. Data are represented as mean ± SEM; 2-tailed Student's t tests for **A**, **B**, **D**, and **F**; 2-way ANOVA tests for **C** and **E**.

human EP4 (EC-hEP4^{OE}) by crossing Tie2-Cre and H11-CAG-loxP-stop-loxP-hEP4 mice (LSL-hEP-4$^{fl/fl}$) (Supplemental Figure 4, A and B). Compared with the LSL-hEP4$^{fl/fl}$ control mice, the EC-hEP4^{OE} mice showed significantly decreased BP at baseline (Figure 4A) and after high-salt diet feeding (Figure 4, B and C). The cardiac function and urine volume were unaltered (Supplemental Figure 4, C–I; and Supplemental Table 2). As in the EC-EP4$^{-/-}$ mice, administration of L-NAME completely eliminated the difference of BP between the LSL-hEP4$^{fl/fl}$ and EC-hEP4^{OE} mice as well (Figure 4, D and E), suggesting increased endothelial production of NO may account for decreased BP levels in the EC-hEP4^{OE} mice. In support, serum NO concentration was significantly higher in the EC-hEP4^{OE} mice than that in control mice (Figure 4F).

EP4 promotes NO production in cultured ECs. To elucidate the molecular mechanism by which EP4 deficiency reduces NO production in ECs, human umbilical vein ECs (HUVECs) and bovine aortic ECs (BAECs) were cultured and treated with the EP4 agonists, including PGE$_1$-OH, CAY10580, and CAY10598. Treatment of HUVECs with PGE$_1$-OH, CAY10580, and CAY10598 markedly promoted NO biosynthesis (Figure 5, A–D; and Supplemental Figure 5, A–H). Similarly, treatment with PGE$_1$-OH and CAY10580 significantly increased NO production in BAECs (Supplemental Figure 5, I and J). Collectively, these findings indicate that EP4 activation can promote NO production in ECs.

Activation of EP4 accelerates eNOS phosphorylation at Ser1177 in ECs. Phosphorylation at Ser1177 (p-eNOS^{Ser1177}) markedly increases the capacity of eNOS to produce NO (17–19). To examine whether EP4 increases eNOS activity in vivo and in vitro, we measured the expression level of total eNOS and p-eNOS^{Ser1177} in the vessels and cultured HUVECs. Although total eNOS protein levels remained unaltered, the p-eNOS^{Ser1177} levels were markedly downregulated in the mesenteric arteries (Figure 5, E and F) and aortas (data not shown) of the EC-EP4$^{-/-}$ mice. In cultured HUVECs, 2 EP4 agonists, PGE$_1$-OH and CAY10580, significantly upregulated the p-eNOS^{Ser1177} levels (Figure 5, G–J). Adenovirus-based overexpression of human EP4 (Ad-hEP4) (Supplemental Figure 5K) resulted in a significant increase of p-eNOS^{Ser1177} levels as well (Figure 5, K and L). However, activation of EP4 did not change eNOS mRNA and total protein levels (Figure 5K and Supplemental Figure 5, L and M). These data demonstrate that EP4 increases NO production largely through the phosphorylation of eNOS at Ser1177.
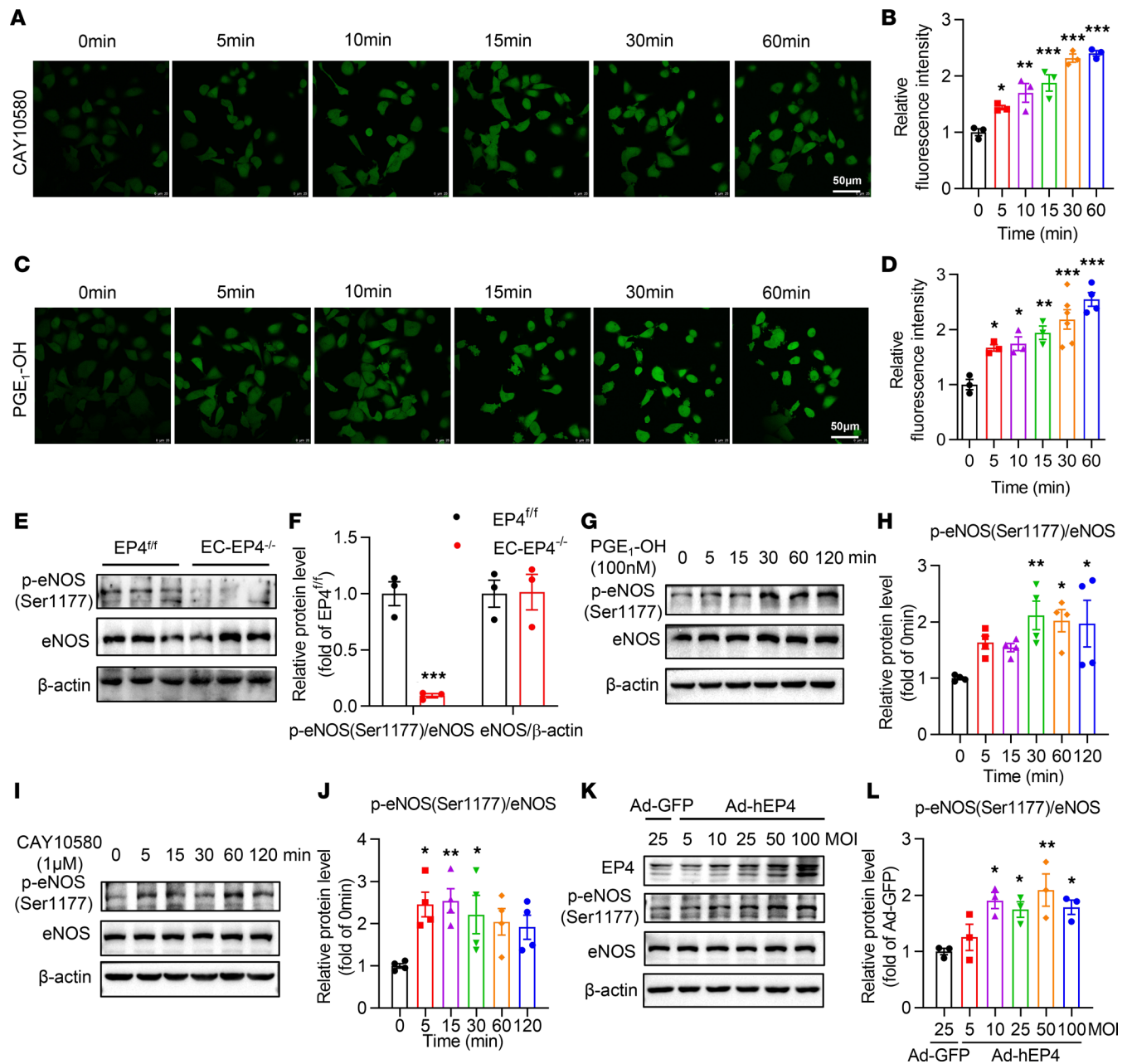
Figure 5. EP4 promotes NO production via enhancing eNOS phosphorylation at Ser1177 in HUVECs. (A and B) The time course (**A**) and the relative fluorescence intensity (**B**) of NO production measured by DAF-FM DA, a NO fluorescence detection probe, in HUVECs treated with CAY10580 (1 μM). *$P < 0.05$, **$P < 0.01$, and ***$P < 0.001$ vs. 0 minutes, $n = 3$. Scale bars: 50 μm. (**C and D**) The time course (**C**) and the relative fluorescence intensity (**D**) of NO production measured by DAF-FM DA in HUVECs treated with PGE$_1$-OH (100 nM). *$P < 0.05$, **$P < 0.01$ and ***$P < 0.001$ vs. 0 minutes, $n = 3$–6. Scale bars: 50 μm. (**E and F**) The protein levels of the p-eNOS at Ser1177 and total eNOS in the mesenteric arteries of the EP4$^{fl/fl}$ and EC-EP4$^{-/-}$ mice. ***$P < 0.001$ vs. EP4$^{fl/fl}$, $n = 3$. (**G and H**) Activation of EP4 by PGE$_1$-OH (100 nM) increased the phosphorylation of eNOS at Ser1177 in a time-dependent manner in HUVECs. *$P < 0.05$, and **$P < 0.01$ vs. 0 minutes, $n = 4$. (**I and J**) Activation of EP4 by CAY10580 (1 μM) increased the phosphorylation of eNOS at Ser1177 in a time-dependent manner in HUVECs. *$P < 0.05$, and **$P < 0.01$ vs. 0 minutes, $n = 4$. (**K and L**) Ad-mediated EP4 overexpression increased the phosphorylation of eNOS at Ser1177 in a dose-dependent manner in HUVECs. The adenovirus was infected for 36 hours. *$P < 0.05$, and **$P < 0.01$ vs. GFP, $n = 3$. Data are represented as mean ± SEM; 1-way ANOVA followed by Dunnett's multiple comparisons tests for **B**, **D**, **H**, **J**, and **L**; 1-way ANOVA followed by Holm-Šidák multiple comparisons test for **F**.

EP4 increases eNOS Ser1177 phosphorylation in an AMPK-dependent manner. Multiple kinases are involved in the phosphorylation of eNOS (20). Among them, AMPK is a major modulator of eNOS activity (21), and its activity is regulated by EP4 (22). To test whether EP4 affects AMPK activity, total and p–AMPK-α (at the Thr172 site) (p-AMPK) levels were determined in the mesenteric arteries of the EC-EP4$^{-/-}$ mice and in HUVECs treated with the EP4 agonists. Deficiency of EP4 in ECs resulted in a
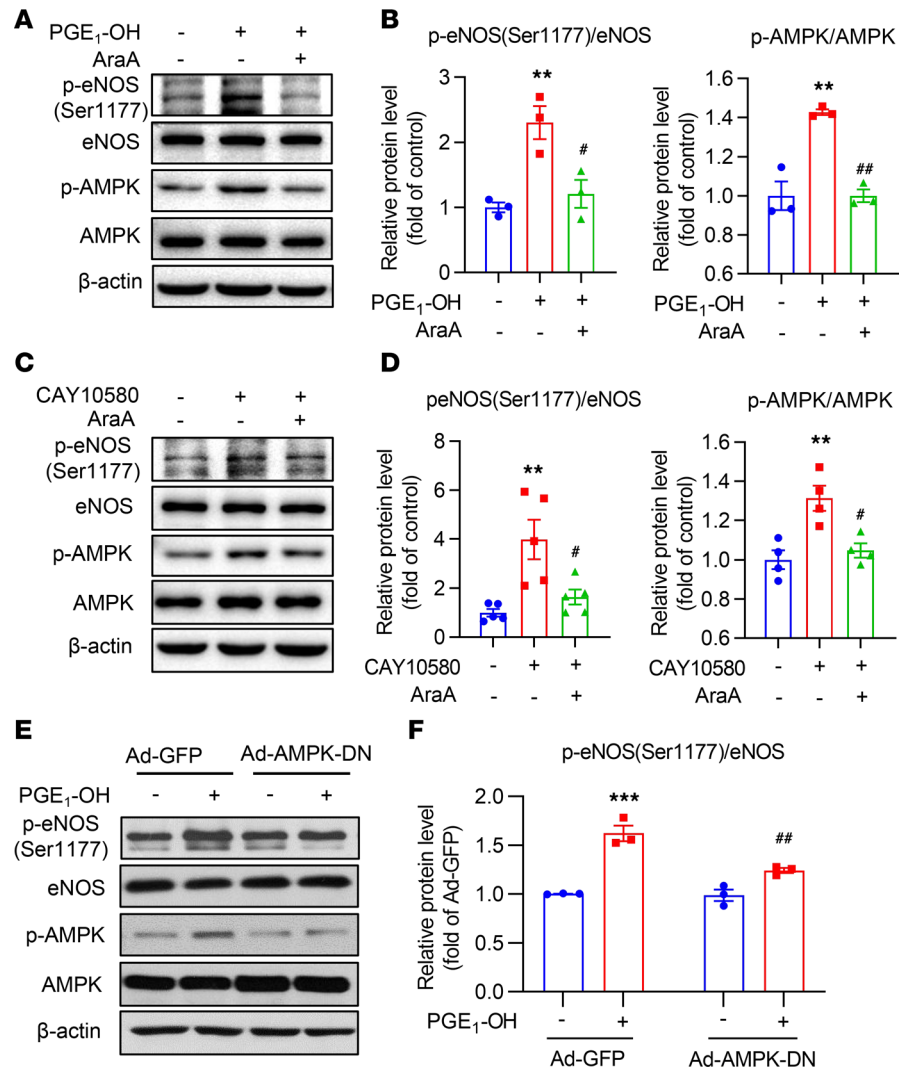
Figure 6. EP4 increases eNOS phosphorylation at Ser1177 via the AMPK pathway. (A and B) The AMPK inhibitor AraA reduced the phosphorylation of eNOS at Ser1177 in HUVECs treated by PGE_1-OH (100 nM) **(A)**. The ratio of p-eNOS to total eNOS and p-AMPK to total AMPK was quantified **(B)**. **$P < 0.01$ vs. control; #$P < 0.05$, and ##$P < 0.01$ vs. PGE_1-OH, $n = 3$. **(C and D)** AraA decreased eNOS phosphorylation at Ser1177 in HUVECs treated with CAY10580 (1 μM) **(C)**. Quantification of the ratio of p-eNOS to total eNOS and p-AMPK to total AMPK was performed **(D)**. **$P < 0.01$ vs. control; #$P < 0.05$ vs. CAY10580, $n = 4$–5. **(E and F)** AMPK inhibition via the infection with an adenovirus containing an AMPK dominant-negative construct (Ad-AMPK-DN) diminished PGE_1-OH–induced eNOS phosphorylation at Ser1177 in HUVECs **(E)**. Quantification of the ratio of p-eNOS to total eNOS is also shown **(F)**. ***$P < 0.001$ vs. GFP; ##$P < 0.01$ vs. GFP + PGE_1-OH, $n = 3$–4. Data are represented as mean ± SEM; 1-way ANOVA followed by Tukey's multiple comparisons tests for **B** and **D**. Two-way ANOVA followed by Tukey's multiple comparisons test for **F**.

significant reduction of activated AMPK (p-AMPK) in the mesenteric arteries (Supplemental Figure 6, A and B), while activation of EP4 by its specific agonists (PGE_1-OH and CAY10580) (Supplemental Figure 6, C–F) and Ad-mediated EP4 overexpression (Supplemental Figure 6, G and H) markedly increased the phosphorylation of AMPK-α at Thr172 site. These results suggest that EP4 deficiency reduces, while EP4 activation enhances, AMPK activity in ECs.

To determine whether AMPK mediates EP4-elicited eNOS activity, we further treated the cells with AraA, an AMPK inhibitor, and found that the EP4 agonist–induced phosphorylation of eNOS at Ser1177 was markedly inhibited (Figure 6, A–D). Similarly, infection with a dominant-negative AMPK adenovirus (Ad-AMPK-DN) (22), which almost completely inhibited PGE_1-OH–induced upregulation of p-AMPK, significantly reduced the p-eNOS[Ser1177] levels (Figure 6, E and F). Moreover, inhibition of AMPK by Ad-AMPK-DN or AraA robustly reduced PGE_1-OH– and Ad-hEP4–elicited
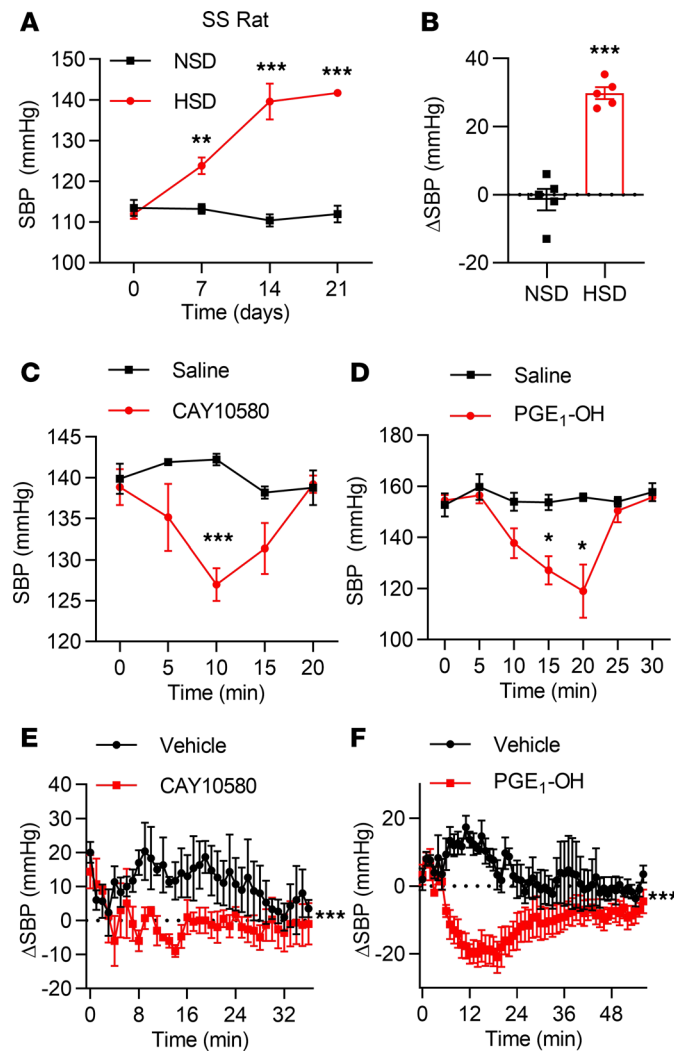
Figure 7. Administration of the EP4 agonists decreases BP in Dahl SS rats. (**A** and **B**) SBP in the SS rats fed with a normal-salt diet (NSD) or a high-salt diet (HSD) (**A**). The net changes of SBP after 3-week diet were compared (**B**). The SBP was monitored by tail cuff. **$P < 0.01$, and ***$P < 0.001$, $n = 5$. (**C** and **D**) Changes of SBP in the SS rats after intraperitoneal injection of CAY10580 (200 μg/kg) (**C**) or PGE$_1$-OH (200 μg/kg) (**D**). The SBP was monitored by tail cuff. *$P < 0.05$, and ***$P < 0.001$, $n = 5$. (**E** and **F**) Net changes of SBP in the SS rats after intraperitoneal injection of CAY10580 (200 μg/kg) (**E**) and PGE$_1$-OH (200 μg/kg) (**F**). The SBP was monitored by telemetry. ***$P < 0.001$, $n = 3$. Data are represented as mean ± SEM; 2-tailed Student's t test for **A**–**D**; 2-way ANOVA tests for **E** and **F**.

NO production (Supplemental Figure 6, I and J). Collectively, these findings illustrate that EP4 promotes NO production mainly via the activation of the AMPK pathway.

EP4 activation decreases BP in Dahl salt-sensitive hypertensive rats. That EP4 gene deficiency increased (Figure 1), while EP4 overexpression in the ECs reduced (Figure 4), BP indicates EP4 may represent an attractive target for the treatment of hypertension. To determine whether pharmacological activation of EP4 decreases BP in hypertensive subjects, Dahl salt-sensitive hypertension rats (SS rats) were used in this study after the induction of hypertension by 2-week high-salt diet treatment, which raised BP from 110 mmHg to 140 mmHg (Figure 7, A and B). Importantly, intraperitoneal administration of PGE$_1$-OH or CAY10580 significantly lowered SBP as measured by both tail-cuff (Figure 7, C and D) and telemetry recording (Figure 7, E and F). Taken together, these results indicate that EP4 activation can effectively decrease BP in hypertensive rodents.

Discussion

Hypertension is the largest preventable contributor to worldwide morbidity and mortality, and improved understanding of its underlying mechanisms could lead to major therapeutic advances (23). NSAIDs are the

most widely used medications as antipyretics, analgesics, and antiinflammatory drugs via inhibiting cyclo-oxygenase (COX-1/2) activity and PG production. However, the clinical use of NSAIDs is associated with many adverse cardiovascular events, especially hypertension (5, 24). Among multiple PGs, PGE_2 is the most abundant prostanoid synthesized in the vasculature and kidney, where it plays a complex role in BP regulation and vascular homeostasis (25, 26). We and others have previously demonstrated that EP1 and EP3 are vasopressors, while EP2 is a vasodepressor agent (8–10). However, the role of EP4 in BP regulation is unclear and remains incompletely understood (27). The present study shows that EC-specific deletion of EP4 increases, while EC-specific overexpression of human EP4 decreases, BP levels in an eNOS/NO-dependent manner. EP4 enhances eNOS activity and increases NO production via an AMPK-dependent mechanism. Our findings demonstrate that endothelial EP4 mediates vasodilation, which is essential for BP homeostasis.

Although the overall systemic effect of PGE_2 is hypotensive, accumulating studies have demonstrated that PGE_2 acts as either a vasodilator or vasoconstrictor depending on which EP receptor is available (8–10, 26). Unlike knockout of the other 3 EP receptors, conventional EP4 knockout is perinatally lethal to mice because of patent ductus arteriosus (28–30). Thus far, the evidence supporting EP4 as a vasorelaxant receptor has largely come from ex vivo pharmacological studies using isolated aortic rings (31, 32). However, in vivo studies give rise to controversial results, with both prohypertensive and antihypertensive actions of EP4 reported (27, 33). To date, the reason for this discrepancy remains largely unknown. Because multiple factors are involved in BP regulation, it is important to dissect the function of EP4 in different tissues and cell types, especially in the vasculature, using genetically manipulated mouse lines with tissue-specific EP4 gene knockout and overexpression.

To study the role of vascular EP4 in BP regulation, we generated 2 potentially novel genetically manipulated mouse lines in whom endogenous EP4 expression was conditionally deleted (EC-EP4$^{-/-}$) or a full-length human EP4 was specifically overexpressed (EC-hEP4^{OE}) in ECs. By using tail-cuff, carotid catheter, and telemetry techniques (34, 35), we found that EC deletion of EP4 led to hypertension, while EC overexpression of human EP4 resulted in hypotension, suggesting an essential role of EC EP4 in BP homeostasis. Because both high-salt diet feeding and chronic AngII infusion resulted in a parallel change in BP in control and the EC-EP4$^{-/-}$ or EC-hEP4^{OE} mice, endothelial EP4 may not contribute to salt and AngII sensitivity, which is in sharp contrast to the findings in mice with VSMC-specific EP4 deletion (VSMC-EP4$^{-/-}$) (11). These findings may imply that endothelial EP4 is critical for basal BP control and targeting endothelial EP4 might represent an effective strategy for the prevention and treatment of hypertension, especially for individuals insensitive to dietary salt intake or less responsive to angiotensin-converting enzyme inhibitor or angiotensin receptor blocker treatment.

The hypertensive phenotype in the EC-EP4$^{-/-}$ mice is attributed to EP4 deficiency in ECs because acute infusion of PGE_2 and an EP4 selective agonist, PGE_1-OH, resulted in less depressor response in the EC-EP4$^{-/-}$ mice. Interestingly, although there was a trend toward BP reduction, no significant difference in hypotensive effect of PGE_2 was observed between controls and the VSMC-EP4$^{-/-}$ mice. This finding is slightly different from a recent report in which acute vasodilatory response to PGE_2 was found to be significantly attenuated in mice with EP4 deficiency in VSMCs (27). In fact, in our study, compared with the EP4$^{fl/fl}$ mice, the VSMC-EP4$^{-/-}$ mice displayed a slightly attenuated (3.6 mmHg) vasodilatory response to PGE_2. The reduction in BP levels is comparable to the approximately 4 mmHg drop Herrera's group found. In addition, the strategy used to specifically delete EP4 in VSMCs was different between the 2 studies. Herrera et al. used mice in whom EP4 was deleted in VSMCs after birth, while in our case, EP4 was prenatally deleted. This may also contribute to the discrepancy. In addition, Herrera et al. demonstrated that although VSMC EP4 may mediate the vasodilatory effects of PGE_2, the protective effect of EP4 on limiting AngII-induced hypertension is unaffected by VSMC EP4 deletion (27), suggesting the expression of EP4 in tissues beyond VSMCs might be responsible for its protective actions in hypertension. In the present study, we provide strong evidence that endothelial EP4, but not VSMC EP4, is essential for BP homeostasis. Expression of EP4 in tissues beyond VSMCs, most likely in ECs, is responsible for its protective actions in hypertension. Taken together, our data clearly, for the first time to our knowledge, suggest that EC, but not VSMC, EP4 is the major contributor to the hypotensive effect of PGE_2.

Although the renin-angiotensin system (RAS), cardiac output, and renal water and sodium excretion are critical for the regulation of BP (36, 37) and EP4 can modulate these physiological processes (12, 38, 39), no difference in plasma renin, AngII, and aldosterone concentrations; urine volume; urinary electrolyte excretion; and cardiac output was observed between control mice and the EC-EP4$^{-/-}$ or EC-hEP4^{OE} mice.

These findings demonstrate that the RAS and cardiac and renal function changes are not involved in the vasodilatory effect of endothelial EP4. Together, the antihypertensive effect of endothelial EP4 very likely results from a direct action on the vasculature.

It has been well documented that impaired endothelial NO production and dysfunction of eNOS activity lead to hypertension (40). In the present study, we found that EC-EP4$^{-/-}$ mice displayed reduced NO production in both plasma and vessels and that EP4 activation significantly increased NO biosynthesis in cultured ECs (Figure 5), suggesting EP4 may lower BP via promoting NO production in the ECs. In support, Ach-elicited vasodilation of the EC-EP4$^{-/-}$ mouse mesenteric arteries was markedly attenuated, and the difference in vasodilatory response to Ach between EC-EP4$^{fl/fl}$ and EC-EP4$^{-/-}$ mice was largely diminished by L-NAME treatment. Importantly, L-NAME treatment almost completely abolished the difference in BP between control mice and EC-EP4$^{-/-}$ or EC-hEP4^{OE} mice. In addition, the altered BP levels in the EC-EP4$^{-/-}$ and EC-hEP4^{OE} mice were not owing to a defect in NO signaling in VSMCs because treatment with SNP, a NO donor, led to a comparable vasorelaxation and BP reduction in control and EC-EP4$^{-/-}$ mice. Collectively, these findings reveal that endothelial EP4 promotes NO production in ECs without affecting NO signaling in VSMCs.

It is well known that multiple kinases can activate eNOS by phosphorylating the Ser1177 residue (p-eNOS^{Ser1177}) or inactivate it by phosphorylating the Thr495 (p-eNOS^{Thr495}) residue (16). In the present study, we found that vascular p-eNOS^{Ser1177} levels were significantly reduced in the EC-EP4$^{-/-}$ mice and that EP4 activation or overexpression markedly increased the p-eNOS^{Ser1177} levels in cultured ECs (Figure 5). In addition, EP4-induced p-eNOS^{Ser1177} expression and NO production were mediated by the activation of AMPK because AMPK inactivation by either AraA or a dominant-negative AMPK vector diminished the effect of EP4. Together, these findings demonstrate that EP4 can increase NO production via increasing the p-eNOS^{Ser1177} level in an AMPK-dependent manner. However, whether EP4 regulates eNOS activity via other signaling pathways remains undetermined. Indeed, the role of the canonical cAMP/PKA pathway in mediating EP4-induced eNOS activity cannot be excluded in the present study.

It has been well documented that control of hypertension is critical in improving cardiovascular and renal outcomes (41). The present study clearly shows that treatment with the EP4 agonists resulted in a substantial decrease in BP in normal mice. Importantly, the EP4 agonist PGE$_1$-OH and CAY10580 markedly reduced BP levels in Dahl salt-sensitive hypertensive rats, as assessed by both tail-cuff and telemetry measurements. These findings suggest that EP4 is a vasodilator and may represent an attractive therapeutic target for the treatment of hypertension.

Notably, although Tie2-Cre mice have been widely used for endothelium-specific gene deletion (42–44), because of mild leakage of Cre activity into the hematopoietic cells (45) and increased vascular inflammation in mice with EP4 deletion in bone marrow–derived cells (46), we cannot absolutely exclude the possibility that bone marrow EP4 might slightly contribute to the phenotypic changes in BP of the EC-EP4$^{-/-}$ mice. To address this issue, we performed ex vivo and in vitro studies by using isolated mesenteric arteries and cultured ECs, respectively. We found that the Ach-induced vasorelaxation was significantly attenuated in the mesenteric arteries isolated from the EC-EP4$^{-/-}$ mice (Figure 2D), and the mesenteric arteries from the EC-EP4$^{-/-}$ mice showed an increased vasoconstrictive response to AngII compared with the EP4$^{fl/fl}$ mice. In addition, treatment with the EP4 agonists markedly promoted NO biosynthesis in cultured HUVECs and in BAECs. Therefore, it is reasonable for us to believe that the increased BP in the EC-EP4$^{-/-}$ mice was largely attributable to the deficiency of EP4-elicited NO production in vascular endothelium but not in bone marrow–derived cells. Nevertheless, further investigations are needed to address this issue with the use of another endothelium-specific Cre driver or the study of these mice following bone marrow transplantations.

Taken together, the present study provides evidence that EP4 promotes NO production via the activation AMPK in the ECs. Deletion of EP4 in the ECs increased, while overexpression of EP4 in the ECs decreased, mouse BP levels. Administration of the EP4 agonists markedly lowered BP in hypertensive rodents. Our data uncover an essential role of endothelial EP4 in BP homeostasis and support a possibility that EP4 activation may represent a new strategy to treat hypertension.

Methods

Generation of the EC-EP4$^{-/-}$ mice. EC-specific EP4 gene–deficient mice were generated using the Cre-loxP system. The Tie2-Cre transgenic mice on 129 background were purchased from The Jackson Laboratory

and backcrossed to C57BL/6 background for 5 generations. EP4-flox/flox mice on C57BL/6 background were generated as previously reported (Supplemental Figure 1) (47).

Generation of the EC-hEP4^{OE} mice. H11 is a ubiquitous locus that permits an exogenous strong promoter inserted within it to drive higher expression. The CRISPR/Cas9 system was used to generate the transgenic mice. A CAG-loxP-stop-loxP-hEP4-flag-polyA segment containing donor vector was made and together with the Cas9 mRNA and sgRNA was coinjected into murine zygotes. The sgRNA directs the Cas9 endonuclease cleavage at the H11 locus and creates a double-strand break, allowing the CAG-loxP-stop-loxP-hEP4-flag-polyA fragment to be inserted into the H11 locus. The LSL-hEP4$^{fl/fl}$ mice were generated on C57BL/6 background. The EC-specific human EP4 overexpression mice (EC-hEP4^{OE}) were then made by crossing the Tie2-Cre transgenic mice with the LSL-hEP4$^{fl/fl}$ mice (Supplemental Figure 4).

High salt–, ʟ-NAME–, and AngII-induced hypertension. For the high-salt diet–induced hypertension condition, the mice received a free intake of a high-salt diet containing 3.5% NaCl (Medicience Ltd.). For the ʟ-NAME–induced hypertension condition, the ʟ-NAME was dissolved in the drinking water at the concentration of 1 g/L. For the AngII-induced hypertension condition, mice were treated with AngII dissolved in sterile saline at 1 μg/kg body weight per minute via a subcutaneously implanted Alzet osmotic minipump (Durect Corp.).

Chemicals and reagents. Primary antibodies against EP4 (catalog 24895-1-AP) and β-actin (catalog 60008-1-Ig) were purchased from Proteintech. Antibodies against p-eNOS^{Ser1177} (Ser1177, catalog 9571), eNOS (catalog 32027), p-AMPK (Thr172, catalog 2535), and AMPK (catalog 2532) were obtained from Cell Signaling Technology. PGE$_2$ (catalog 14010), PGE$_1$-OH (catalog 13020), CAY10580 (catalog 16835), CAY10598 (catalog 13281), sulprostone (catalog 14765), and butaprost (catalog 13740) were purchased from Cayman Chemical. ʟ-NAME (catalog N5751), phenylephrine (catalog P1250000), Ach (catalog A6625), SNP (catalog BP453), AraA (catalog A5762), and DAF-FM DA (catalog D1946) were purchased from MilliporeSigma. AngII (catalog HY-13948) was purchased from MedChemExpress.

Tail cuff BP measurements. A noninvasive tail-cuff device (BP-2010 series BP meter, Softron) was used to measure SBP in mice and rats. Male mice (8–12 weeks old, body weight 25–35 g) and rats (8–12 weeks old, body weight 250–300 g) were used for BP measurement. The animals were pretrained for 2 weeks to fully adapt to the environment and procedure. Before recording, the mouse or rat had a rest for no less than 10 minutes until the animal remained comfortably and quietly in the holder. SBP was recorded at 1300 hours as previously reported (11).

Direct measurement of carotid arterial BP. For acute infusion studies, mice were anesthetized with 80 mg/kg ketamine and 8 mg/kg inactin i.p. and placed on a thermostatic operating table. After disinfection, a PE10 catheter was inserted into the right carotid artery, and the contralateral jugular vein was opened for fluid infusion. BP was measured with a transducer connected with a Cobe CDX II transducer connected to a BP analyzer (BPA 400; Micromed) as previously reported (11). PGE$_2$ (100 μg/kg), PGE$_1$-OH (100 μg/kg), or CAY10580 (100 μg/kg) was intravenously administered, and arterial BP was directly recorded for 15 minutes after the drug injection.

BP recording via implantable radio telemetry. BP was measured continuously in conscious and freely moving mice using radio telemetry (DSI, MN55112), as described previously (27). Male mice (8–12 weeks old, 25–35 g) were anesthetized by phenobarbital (60 μg/g, i.p.) and placed on a thermostatic operating pad. After the operation, the implantable (HD-11X series) BP-measuring catheter was inserted into the left carotid artery, and the device was fixed under the skin of the back of the mouse before suturing. For Dahl SS rats (8–12 weeks old, body weight 250–300 g), a catheter was inserted into the abdominal aorta after anesthesia, and the device was fixed under the rectus abdominis. These experimental animals were subjected to 14 days of postoperative recovery to fully adapt to the implants.

Vascular tension assay of the mesenteric arteries. The mesenteric arteries were isolated from male EP4$^{fl/fl}$ and EC-EP4$^{-/-}$ mice after sacrifice with CO$_2$ and cut into rings of about 2 mm long in ice-cold modified Krebs-Ringer bicarbonate buffer, as previously reported (48). Each segment was suspended between 2 tungsten wires in chambers of a Multi Myograph System (610M, Danish Myo Technology A/S) for the measurement of isometric force. Each organ chamber was filled with 5 mL of the modified Krebs-Ringer bicarbonate solution maintained at 37°C ± 0.5°C and aerated with 95% O$_2$ and 5% CO$_2$ (pH = 7.4). At the beginning of the experiment, each vessel ring was stretched to its optimal resting tension of 1 mN for 30 minutes by stepwise stretching and contracted with 60 mM KCl to test its contractility. Vessels were brought to their optimal resting tension and equilibrated for 30 minutes, and a dose response to AngII, phenylephrine, Ach, and SNP in vessels was determined. To inhibit NO production, ʟ-NAME (100 μM) was preincubated for 30 minutes.

Echocardiography. For in vivo ultrasound images, cardiac function parameters were monitored in isoflurane-anesthetized mice (2% isoflurane) by high-frequency ultrasound with a VEVO 3100 echography device (VisualSonics) with 30-μm resolution. The images were measured using VEVO 3100 software (version 1.5.0).

Cell culture and drug treatment. HUVECs were isolated from umbilical cords and cultured in Medium 199 (Thermo Fisher Scientific) containing 20% FBS, 20 mmol/L HEPES (pH 7.4), 5 ng/mL recombinant human fibroblast growth factor, 90 μg/mL heparin, and antibiotics in a humidified 5% CO_2, 37°C incubator (Thermo Fisher Scientific). Experiments on HUVECs were carried out at passages 3–7. BAECs were cultured in RPMI-1640 (Thermo Fisher Scientific) with 10% FBS and antibiotics in a humidified 5% CO_2, 37°C incubator.

Measurement of intracellular NO. After the indicated treatment, HUVECs were lysed by the lysis buffer (Cell and Tissue Lysis Buffer for Nitric Oxide Assay, Beyotime Institute of Biotechnology) for the measurement of the intracellular levels of NO in the supernatant using the Total Nitric Oxide Detection Kit (Beyotime Institute of Biotechnology) according to the manufacturer's instructions. HUVECs or BAECs were also loaded with the NO indicator DAF-FM DA (10 μg/mL) in PBS for 30 minutes in the dark at 37°C. After being washed to remove excess indicator, cells were imaged in PBS using a Leica SP8 Live inverted confocal microscope with the excitation laser at 488 nm and 506–526 nm emission.

Western blot analysis and real-time PCR. For Western blot analysis, the cells were lysed in a RIPA buffer containing protease inhibitor cocktail (HY-K0010, MedChemExpress). After centrifugation at 12,000 *g* for 15 minutes, total protein was quantified by a BCA Protein Assay Kit (Thermo Scientific). Cell lysates were mixed with SDS-PAGE loading buffer, fractionated with 10% SDS-PAGE, and transferred onto nitrocellulose filter membranes. The membranes were then incubated with the primary antibodies overnight at 4°C, followed by incubation with secondary antibody for 1 hour at room temperature. Finally, the membranes were incubated with SuperLumia ECL Plus HRP Substrate Reagent, and signals from immunoreactive bands were visualized using a Chemiluminescent Imaging System (Tanon 5200).

For real-time PCR, total RNA was extracted by TRIzol reagent (Thermo Fisher Scientific), quantified by NanoDrop 2000 (Thermo Fisher Scientific), and reverse-transcribed to cDNA. Primers were designed from the known sequences of mouse genes or human genes listed in Supplemental Table 3. We used β-actin as an internal standard. SYBR Green (Invitrogen, Thermo Fisher Scientific) was used as fluorochrome according to the manufacturer's instructions. The PCR was performed on the ABI 7300 plus system using reactions of 94°C for 5 minutes, then 35 cycles of 94°C for 30 seconds, 59°C for 30 seconds, and 72°C for 30 seconds, followed by extension at 72°C for 5 minutes.

Statistics. All results are presented as mean ± SEM. Statistical analyses were performed using Graph-Pad Prism 8.3.0 software. Details of the statistical tests are indicated in the figure legends. $P < 0.05$ was considered significant.

Study approval. All animal experiments were reviewed and approved by the Animal Care and Use Review Committee of Dalian Medical University. The study conformed to the *Guide for the Care and Use of Laboratory Animals* published by the US NIH (NIH publication no. 85-23, revised 1996).

Author contributions

HX conceived the study, designed the methodology, performed formal analysis, and wrote the original draft. BF validated results and investigated. SD designed the methodology and performed formal analysis. SW designed the methodology and validated results. QL, XJ, CB, LY, XS, LQ, and ZL investigated. GY visually represented data. FZ and NW provided resources. LC, XZ, and YG reviewed and edited the draft and administered and supervised the project. HX, BF, and SD had equal intellectual contributions, and their order as co–first authors was determined by the amount of time they contributed. All authors revised the manuscript and gave final approval for publication.

Acknowledgments

Address correspondence to: Lihong Chen, Xiaoyan Zhang, or Youfei Guan, the Advanced Institute for Medical Sciences, Dalian Medical University, No. 9, West Section, Lvshun South Road, Dalian, 116044, China. Phone: 86.041186118984; Email: lihong@dmu.edu.cn (LC). Phone: 86.041186118983; Email: wserien@163.com (XZ). Phone: 86.041186110021; Email: guanyf@dmu.edu.cn (YG).

1. Elliott WJ. Systemic hypertension. *Curr Probl Cardiol*. 2007;32(4):201–259.
2. Safar ME, et al. Interaction between hypertension and arterial stiffness. *Hypertension*. 2018;72(4):796–805.
3. Fleming I. Molecular mechanisms underlying the activation of eNOS. *Pflugers Arch*. 2010;459(6):793–806.
4. Poulos TL, Li H. Nitric oxide synthase and structure-based inhibitor design. *Nitric Oxide*. 2017;63:68–77.
5. Smyth EM, Grosser T, Wang M, Yu Y, FitzGerald GA. Prostanoids in health and disease. *J Lipid Res*. 2009;50(suppl):S423–S428.
6. Hatae N, Sugimoto Y, Ichikawa A. Prostaglandin receptors: advances in the study of EP3 receptor signaling. *J Biochem*. 2002;131(6):781–784.
7. Yokoyama U, Iwatsubo K, Umemura M, Fujita T, Ishikawa Y. The prostanoid EP4 receptor and its signaling pathway. *Pharmacol Rev*. 2013;65(3):1010–1052.
8. Chen L, et al. Inactivation of the E-prostanoid 3 receptor attenuates the angiotensin II pressor response via decreasing arterial contractility. *Arterioscler Thromb Vasc Biol*. 2012;32(12):3024–3032.
9. Kennedy CR, et al. Salt-sensitive hypertension and reduced fertility in mice lacking the prostaglandin EP2 receptor. *Nat Med*. 1999;5(2):217–220.
10. Guan Y, et al. Antihypertensive effects of selective prostaglandin E2 receptor subtype 1 targeting. *J Clin Invest*. 2007;117(9):2496–2505.
11. Xu H, et al. VSMC-specific EP4 deletion exacerbates angiotensin II-induced aortic dissection by increasing vascular inflammation and blood pressure. *Proc Natl Acad Sci U S A*. 2019;116(17):8457–8462.
12. Zhu L, et al. The cyclooxygenase-1/mPGES-1/endothelial prostaglandin EP4 receptor pathway constrains myocardial ischemia-reperfusion injury. *Nat Commun*. 2019;10(1):1888.
13. Hao H, et al. Protective role of mPGES-1 (microsomal prostaglandin E synthase-1)-derived PGE_2 (prostaglandin E_2) and the endothelial EP4 (prostaglandin E receptor) in vascular responses to injury. *Arterioscler Thromb Vasc Biol*. 2018;38(5):1115–1124.
14. Rajapakse NW, Mattson DL. Role of cellular L-arginine uptake and nitric oxide production on renal blood flow and arterial pressure regulation. *Curr Opin Nephrol Hypertens*. 2013;22(1):45–50.
15. Umans JG, Levi R. Nitric oxide in the regulation of blood flow and arterial pressure. *Annu Rev Physiol*. 1995;57:771–790.
16. Tejero J, Shiva S, Gladwin MT. Sources of vascular nitric oxide and reactive oxygen species and their regulation. *Physiol Rev*. 2019;99(1):311–379.
17. Fleming I, Busse R. Molecular mechanisms involved in the regulation of the endothelial nitric oxide synthase. *Am J Physiol Regul Integr Comp Physiol*. 2003;284(1):R1–12.
18. McCabe TJ, Fulton D, Roman LJ, Sessa WC. Enhanced electron flux and reduced calmodulin dissociation may explain "calcium-independent" eNOS activation by phosphorylation. *J Biol Chem*. 2000;275(9):6123–6128.
19. Mount PF, Kemp BE, Power DA. Regulation of endothelial and myocardial NO synthesis by multi-site eNOS phosphorylation. *J Mol Cell Cardiol*. 2007;42(2):271–279.
20. Garcia V, Sessa WC. Endothelial NOS: perspective and recent developments. *Br J Pharmacol*. 2019;176(2):189–196.
21. Morrow VA, Foufelle F, Connell JM, Petrie JR, Gould GW, Salt IP. Direct activation of AMP-activated protein kinase stimulates nitric-oxide synthesis in human aortic endothelial cells. *J Biol Chem*. 2003;278(34):31629–31639.
22. Zhu Z, et al. Prostaglandin E2 promotes endothelial differentiation from bone marrow-derived cells through AMPK activation. *PLoS One*. 2011;6(8):e23554.
23. GBD 2015 Risk Factors Collaborators. Global, regional, and national comparative risk assessment of 79 behavioural, environmental and occupational, and metabolic risks or clusters of risks, 1990-2015: a systematic analysis for the Global Burden of Disease Study 2015. *Lancet*. 2016;388(10053):1659–1724.
24. Solomon SD. Cyclooxygenase-2 inhibitors and cardiovascular risk. *Curr Opin Cardiol*. 2006;21(6):613–617.
25. Wang J, Liu M, Zhang X, Yang G, Chen L. Physiological and pathophysiological implications of PGE_2 and the PGE_2 synthases in the kidney. *Prostaglandins Other Lipid Mediat*. 2018;134:1–6.
26. Yang T, Du Y. Distinct roles of central and peripheral prostaglandin E2 and EP subtypes in blood pressure regulation. *Am J Hypertens*. 2012;25(10):1042–1049.
27. Herrera M, Yang T, Sparks MA, Manning MW, Koller BH, Coffman TM. Complex role for E-prostanoid 4 receptors in hypertension. *J Am Heart Assoc*. 2019;8(4):e010745.
28. Segi E, et al. Patent ductus arteriosus and neonatal death in prostaglandin receptor EP4-deficient mice. *Biochem Biophys Res Commun*. 1998;246(1):7–12.
29. Schneider A, et al. Generation of a conditional allele of the mouse prostaglandin EP4 receptor. *Genesis*. 2004;40(1):7–14.
30. Nguyen M, et al. The prostaglandin receptor EP4 triggers remodelling of the cardiovascular system at birth. *Nature*. 1997;390(6655):78–81.
31. Zhang Y, Guan Y, Schneider A, Brandon S, Breyer RM, Breyer MD. Characterization of murine vasopressor and vasodepressor prostaglandin E(2) receptors. *Hypertension*. 2000;35(5):1129–1134.
32. Hristovska AM, et al. Prostaglandin E2 induces vascular relaxation by E-prostanoid 4 receptor-mediated activation of endothelial nitric oxide synthase. *Hypertension*. 2007;50(3):525–530.
33. Wang F, et al. Prostaglandin E-prostanoid4 receptor mediates angiotensin II-induced (pro)renin receptor expression in the rat renal medulla. *Hypertension*. 2014;64(2):369–377.
34. Luft FC. Men, mice, and blood pressure: telemetry? *Kidney Int*. 2019;96(1):31–33.
35. Luther JM, Fogo AB. Under pressure-how to assess blood pressure in rodents: tail-cuff? *Kidney Int*. 2019;96(1):34–36.

36. van Thiel BS, van der Pluijm I, te Riet L, Essers J, Danser AH. The renin-angiotensin system and its involvement in vascular disease. *Eur J Pharmacol*. 2015;763(pt A):3–14.

37. Magder S. The meaning of blood pressure. *Crit Care*. 2018;22(1):257.

38. Schnermann J, Briggs JP. Synthesis and secretion of renin in mice with induced genetic mutations. *Kidney Int*. 2012;81(6):529–538.

39. Facemire CS, et al. A major role for the EP4 receptor in regulation of renin. *Am J Physiol Renal Physiol*. 2011;301(5):F1035–F1041.

40. Huang PL, et al. Hypertension in mice lacking the gene for endothelial nitric oxide synthase. *Nature*. 1995;377(6546):239–242.

41. Whelton PK, et al. 2017 ACC/AHA/AAPA/ABC/ACPM/AGS/APhA/ASH/ASPC/NMA/PCNA Guideline for the Prevention, Detection, Evaluation, and Management of High Blood Pressure in Adults: Executive Summary: a report of the American College of Cardiology/American Heart Association Task Force on Clinical Practice Guidelines. *Hypertension*. 2018;71(6):1269–1324.

42. Wang L, et al. Integrin-YAP/TAZ-JNK cascade mediates atheroprotective effect of unidirectional shear flow. *Nature*. 2016;540(7634):579–582.

43. Maliken BD, et al. Gata4-dependent differentiation of c-Kit+-derived endothelial cells underlies artefactual cardiomyocyte regeneration in the heart. *Circulation*. 2018;138(10):1012–1024.

44. Špiranec K, et al. Endothelial C-type natriuretic peptide acts on pericytes to regulate microcirculatory flow and blood pressure. *Circulation*. 2018;138(5):494–508.

45. Tang Y, Harrington A, Yang X, Friesel RE, Liaw L. The contribution of the Tie2+ lineage to primitive and definitive hematopoietic cells. *Genesis*. 2010;48(9):563–567.

46. Tang EH, et al. Deletion of EP4 on bone marrow-derived cells enhances inflammation and angiotensin II-induced abdominal aortic aneurysm formation. *Arterioscler Thromb Vasc Biol*. 2011;31(2):261–269.

47. Gao M, et al. Disruption of prostaglandin E2 receptor EP4 impairs urinary concentration via decreasing aquaporin 2 in renal collecting ducts. *Proc Natl Acad Sci U S A*. 2015;112(27):8397–8402.

48. Wang X, et al. Nuciferine relaxes rat mesenteric arteries through endothelium-dependent and -independent mechanisms. *Br J Pharmacol*. 2015;172(23):5609–5618.